PHYSICAL REVIEW B **77**, 134408 (2008)

Magnetic double-q ordering of tetragonal $GdNi_2B_2C$: A way to explain the magnetoelastic paradox

Jens Jensen[1] and Martin Rotter[2]

[1]Niels Bohr Institute, Universitetsparken 5, 2100 Copenhagen, Denmark

[2]Institut für Physikalische Chemie, Universität Wien, Währingerstrasse 42, 1010 Wien, Austria

(Received 20 December 2007; revised manuscript received 13 February 2008; published 2 April 2008)

The orbital contribution to the magnetic moment of Gd^{3+} is zero, and the anisotropy is weak and dominated by the classical dipole interaction in most Gd systems. At the ordering wave vector $\boldsymbol{q} \simeq (0.55,0,0)$ in $GdNi_2B_2C$, the transverse b components are more strongly coupled than the a and c components, and the magnetic moments order in a linearly polarized sinusoidal wave just below T_N. In this situation, the fourth-order term in the Landau expansion favors the double-q ordering, which ordering is found to explain the magnetic phase diagram and the "magnetoelastic paradox."

DOI: 10.1103/PhysRevB.77.134408 PACS number(s): 75.80.+q, 75.25.+z, 74.70.Dd

I. INTRODUCTION

The ground state of the Gd^{3+} ion is a pure S multiplet, $J=S=7/2$ and $g=2$, and, generally, the magnetic anisotropy of a Gd compound is an order of magnitude smaller than that in compounds with other rare-earth ions. The separation between Hund's ground state and the higher multiplets is large, and the single-ion anisotropy due to the crystal-field mixing of multiplets may probably be neglected compared to the anisotropy deriving from spin-orbit modifications of the exchange interaction between neighboring spins. Although this exchange anisotropy is a possibility, the indications are that the anisotropy in many Gd compounds is dominated by the classical dipole-dipole interaction.[1,2] In this case, the magnetic Hamiltonian is the sum of a Heisenberg exchange term and the classical dipole interaction,

$$\mathcal{H} = -\frac{1}{2}\sum_{ij} \mathcal{J}_{ij}\boldsymbol{J}_i \cdot \boldsymbol{J}_j - \frac{1}{2}\sum_{ij}\sum_{\alpha\beta} \mathcal{J}_D D_{ij}^{\alpha\beta} J_{i\alpha}J_{j\beta}. \tag{1}$$

The dipole coupling parameter is $\mathcal{J}_D=(g\mu_B)^2N$, where N is the number of Gd ions per unit volume and

$$D_{ij}^{\alpha\beta} = \frac{3(r_{i\alpha}-r_{j\alpha})(r_{i\beta}-r_{j\beta}) - |\boldsymbol{r}_i-\boldsymbol{r}_j|^2\delta_{\alpha\beta}}{N|\boldsymbol{r}_i-\boldsymbol{r}_j|^5}. \tag{2}$$

$GdNi_2B_2C$ belongs to the series of rare-earth borocarbides RNi_2B_2C. The interest for this series of intermetallic compounds stems from the unusual property that four of the members (R=Tm,Er,Ho,Dy) show coexistence of superconductivity and antiferromagnetic ordering.[3,4] Neutron-diffraction, nuclear magnetic resonance, and other experimental studies of the borocarbides suggest the presence of antiferromagnetic fluctuations related to the $3d$ electrons of the Ni ions, but the time-averaged moments on the Ni sites are found to be vanishing small.[3–6] The absence of static Ni moments implies that the $3d$ electrons only affect the magnetic properties of these compounds in an indirect way via their influence on the Ruderman–Kittel–Kasuya–Yoshida (RKKY) interaction. In other words, with respect to the magnetic properties, the borocarbides may be characterized as being pure $4f$ systems.

Although $GdNi_2B_2C$ does not become superconducting, it is of particular importance to understand the magnetic properties of this compound since it does not share the extra complexities deriving from the strong anisotropy effects detected in the other heavy-rare-earth borocarbides. Important examples are the commensurable lock-in effects in the Er compound[7,8] and the additional quadrupolar ordering of Tm borocarbide that has recently been discovered.[9] The crystal structure of the borocarbides is tetragonal ($I4/mmm$) and the rare-earth ions are placed on a body-centered lattice. In the Gd case, $a=3.574$ Å and $c=10.366$ Å, implying $\mathcal{J}_D=3.243$ μeV. The Néel temperature of $GdNi_2B_2C$ is $T_N=19.4$ K. The magnetic ordering has been studied by magnetic x-ray scattering on single crystals[10] and by hot-neutron diffraction of a polycrystalline sample.[11] The ordering wave vector $\boldsymbol{q} \simeq (0.55,0,0)$ (in reciprocal lattice units) is about the same as in the Er and Tb borocarbides.[5] The most important interaction between the localized rare-earth moments is the indirect RKKY coupling mediated by the conduction electrons, and band-structure calculations indicate that nesting effects are important close to (0.55,0,0).[12] From the x-ray experiments,[10] it is concluded that the polarization of the ordered moments in $GdNi_2B_2C$ is linear between $T_N=19.4$ K and $T_R=13.6$ K, with the moments being along the transverse b axis. Below T_R, the moments develop a component along the c axis. The diffraction experiments do not determine the phase angle difference between the two components, but the model calculations presented below leave no doubt that the polarization is elliptical.

The phase diagram in the presence of a field applied along the a or along the c axis has been determined by El Massalami *et al.*[13] from observations of kinks in the magnetization or magnetostriction measurements. The results obtained, when applying the field along the c axis, show the expected two phase lines, one at the field at which the polarization changes between an elliptical and a linear one and one between the antiferromagnetic and the paramagnetic phase. The a-axis measurements showed an additional low-field phase line, which El Massalami *et al.* interpreted as a domain alignment transition. The star of four equivalent ordering wave vectors $(\pm 0.55,0,0)$ and $(0,\pm 0.55,0)$ implies the presence of two domains, if the ordering is assumed to be

©2008 The American Physical Society

single q. The domain in which the moments are perpendicular to the a-axis field is then favored by the field.

Because of the weakness of the anisotropy, the magnetostrictive strains observed in Gd compounds mostly derive from the exchange interaction,[14] and the deformations induced by the magnetic ordering are only of the order of 10^{-4} in $\mathrm{GdNi_2B_2C}$. As discussed in Ref. 11, the strain dependence of the RKKY interaction may lead to symmetry preserving α strains but also to an orthorhombic distortion of the tetragonal plane,

$$\epsilon_a - \epsilon_b \propto \frac{1}{N}\sum_i \langle \boldsymbol{J}(\boldsymbol{r}_i)\cdot\boldsymbol{J}(\boldsymbol{r}_i+\boldsymbol{a}) - \boldsymbol{J}(\boldsymbol{r}_i)\cdot\boldsymbol{J}(\boldsymbol{r}_i+\boldsymbol{b})\rangle, \tag{3}$$

where the correlation function is nonzero in the antiferromagnetic phase but vanishes for a para- or ferromagnet. In general, the symmetry-breaking zero-field distortions anticipated in antiferromagnetic Gd compounds are found to be vanishing small compared to symmetry preserving α strains, which is named the "magnetoelastic paradox."[11] However, in the present system, the orthorhombic distortion is occurring, not at zero field but in the presence of an applied field along the a axis larger than the "domain-alignment field." Just above this field, the observed distortion is at its maximum, and it is gradually reduced as the paramagnetic phase is approached. In Ref. 11, it was shown that the relative variation of $\epsilon_a - \epsilon_b$ as a function of the a-axis field is well accounted for by the correlation function in Eq. (3) at fields larger than the "domain-alignment field," but the reversible vanishing of the distortion in the zero-field limit was left unexplained.

II. MEAN-FIELD ANALYSIS AND THE LANDAU EXPANSION

In the mean-field approximation, the Hamiltonian in Eq. (1) leads to a free energy, which to fourth order in the magnetization is[2]

$$F = -Nk_BT\ln(2J+1) - \frac{1}{2}\sum_{ij}\sum_{\alpha\beta}\mathcal{J}_{ij}^{\alpha\beta}\langle J_{i\alpha}\rangle\langle J_{j\beta}\rangle + \sum_i [A|\langle \boldsymbol{J}_i\rangle|^2 + B|\langle \boldsymbol{J}_i\rangle|^4 - g\mu_B\boldsymbol{H}\cdot\langle \boldsymbol{J}_i\rangle], \tag{4}$$

where $\mathcal{J}_{ij}^{\alpha\beta} \equiv \mathcal{J}_{ij} + \mathcal{J}_D D_{ij}^{\alpha\beta}$ and

$$A = \frac{3k_BT}{2J(J+1)}, \quad B = \frac{9}{20}\frac{J^2+J+\frac{1}{2}}{J^3(J+1)^3}k_BT. \tag{5}$$

The additional magnetoelastic contributions are of the order of 10^{-3} meV per Gd ion and thus negligible in comparison with the terms in Eq. (4). The maximum in the Fourier transform $\mathcal{J}^{\alpha\beta}(\boldsymbol{q})$ of the two-ion interaction $\mathcal{J}_{ij}^{\alpha\beta}$ occurs at $\boldsymbol{q}_1 = (0.55,0,0)$ and $\boldsymbol{q}_2 = (0,0.55,0)$, at which vectors the interaction is diagonal. All three diagonal elements are different from each other because of the classical dipole coupling. The longitudinal component is generally suppressed (most strongly at long wavelengths) and because $c > a$, the cc component is smaller than the transverse one within the a-b plane. Hence, the maximum value is $\mathcal{J}^{bb}(\boldsymbol{q}_1) = \mathcal{J}^{aa}(\boldsymbol{q}_2)$. In this situation, the free-energy expression predicts a sinusoidal ordering of the b or the a component of $\langle \boldsymbol{J}_i\rangle$ at the wave vector $\boldsymbol{q}_1$ or $\boldsymbol{q}_2$, respectively, when the temperature is slightly below $T_N = J(J+1)\mathcal{J}^{bb}(\boldsymbol{q}_1)/(3k_B)$. Assuming a superposition of the two possibilities,

$$\langle \boldsymbol{J}_i\rangle = (m_a\cos(\boldsymbol{q}_2\cdot\boldsymbol{r}_i+\phi_a), m_b\cos(\boldsymbol{q}_1\cdot\boldsymbol{r}_i+\phi_b), 0), \tag{6}$$

the free energy per Gd ion at zero field is found to be

$$\frac{F}{N} = -k_BT\ln(2J+1) + \frac{1}{4}[2A - \mathcal{J}^{bb}(\boldsymbol{q}_1)](m_a^2+m_b^2) + B\left[\frac{3}{8}(m_a^2+m_b^2)^2 - \frac{1}{4}m_a^2m_b^2\right]. \tag{7}$$

Written in this way, the last negative term of fourth order immediately shows that the free energy is minimized when $m_a = m_b$. The double-q structure leads effectively to a smaller site variation of $|\langle \boldsymbol{J}_i\rangle|$ compared to the single-q case. The most effective minimization of $|\langle \boldsymbol{J}_i\rangle|$ is achieved by the helix. If the a-axis component in Eq. (6) is being replaced by a c-axis component equal to $m_b\sin(\boldsymbol{q}_1\cdot\boldsymbol{r}_i+\phi_b)$, the last negative term in Eq. (7) becomes twice as large, but this helical ordering is suppressed close to T_N by the second-order terms since $\mathcal{J}^{cc}(\boldsymbol{q}_1) < \mathcal{J}^{bb}(\boldsymbol{q}_1)$ in the present system.

The extra entropy gain of the helix compared to the linearly polarized ordering is well established,[2] but it is less commonly known that the double-q structure of two linearly polarized ordered waves is able to reduce the site variation of $|\langle \boldsymbol{J}_i\rangle|$. The present case shares similarities with the cubic compound $\mathrm{CeAl_2}$, where the double-q structure is also found to be stable.[15] The reduction of the free energy of the double-q structure depends on the angle between the two polarization vectors. If this angle is θ, then the fourth-order term in Eq. (7), $-B\frac{1}{4}m_a^2m_b^2$, is being replaced by $B(\cos^2\theta - \frac{1}{4})m_a^2m_b^2$. This fourth-order term vanishes in the case of dhcp Nd metal, where the angle is $\frac{2\pi}{3}$, but the term nevertheless stabilizes a double-q ordering of Nd less than 1 K below the single-q transition, in which structure the two polarization vectors are rotated an angle of probably up to about 24° toward each other. This circumstance was first realized by Forgan[16] (see also Ref. 21 and Sec. 2.1.6 of Ref. 2).

The Landau expansion in Eq. (4) may be used for estimating the critical a-axis fields close to T_N,

$$H(1q) = 3H(2q) = \left[\frac{5}{3}\frac{(J+1)^2}{J^2+J+\frac{1}{2}}\frac{T_N - T}{T_N}\right]^{1/2} H(0), \tag{8}$$

where $H(0)$ is the critical (internal) a-axis field at zero temperature,

$$g\mu_BH(0) = J[\mathcal{J}^{bb}(\boldsymbol{q}_1) - \mathcal{J}^{aa}(\boldsymbol{0})]. \tag{9}$$

The double-q structure disappears at the field $H(2q)$, above which the single-q structure, with m_b being nonzero, stays stable up to the three times larger field $H(1q)$.

At lower temperatures, the situation becomes more complex and, instead of making further use of the Landau expansion, we have performed a numerical analysis of a mean-field model for $\mathrm{GdNi_2B_2C}$. Part of the calculations were done using the MCPHASE[17] program package.[18–20] We list some technical details:

TABLE I. The exchange coupling parameters used in the model calculations of $GdNi_2B_2C$. n is the number of equivalent neighbors.

$\boldsymbol{r}_{ij}$	n	$\lvert\boldsymbol{r}_{ij}\rvert$ (Å)	$\mathcal{J}_{ij}$ (μeV)
(1, 0, 0)	4	3.57	49.9
(1, 1, 0)	4	5.05	−71.7
$(\frac{1}{2},\frac{1}{2},\frac{1}{2})$	8	5.77	−21.6
$(\frac{3}{2},\frac{1}{2},\frac{1}{2})$	16	6.10	2.2
(2, 0, 0)	4	7.15	−10.0
(2, 1, 0)	8	7.99	16.1
(0, 0, 1)	2	10.37	15.0

Most of the calculations were done on, effectively, a centered square lattice by assuming the commensurable period to consist of $9\times9\times2$ uniform atomic chains perpendicular to the a-b plane corresponding to $|\boldsymbol{q}_1|=\frac{5}{9}$, but $|\boldsymbol{q}_1|=\frac{6}{11}$ has also been used at low fields and temperatures.

The exchange parameters of the final fit are given in Table I, and Fig. 1 shows the Fourier transform of the total two-ion interaction tensor, when $\boldsymbol{q}$ is along [100]. In this case, only the diagonal components are nonzero: $\mathcal{J}^{\alpha\alpha}(\boldsymbol{q}) = \mathcal{J}(\boldsymbol{q})+\mathcal{J}_D D^{\alpha\alpha}(\boldsymbol{q})$ with $\alpha=a$, b, or c.

The effective interaction parameters of the classical dipole coupling between the sites of a commensurable period may be calculated accurately by summing over tens of periods in the a-b plane and hundreds of layers along the c axis. The convergence is extremely slow in the long wavelength limit but only the values at $q\equiv0$ need to be corrected because only a discrete number of Fourier components are involved in the case of a commensurable structure. The classical contribution is of the order of 10% of the exchange interaction leading to significant differences between the three components of $\mathcal{J}^{\alpha\alpha}(\boldsymbol{q})$ at the ordering wave vector $\boldsymbol{q}_1$, as shown in Fig. 1.

In all the calculations, the sample was assumed to be a sphere, and including the demagnetization field in the Zeeman term, then H in Eq. (4) is the internal field. With this choice,[2] the transverse components, $\mathcal{J}^{bb}[(q,0,0)]$ and $\mathcal{J}^{cc}[(q,0,0)]$ in Fig. 1, behave smoothly in the long wavelength limit, whereas the longitudinal one $\mathcal{J}^{aa}[(q,0,0)]|_{q\to0}=\mathcal{J}^{aa}(\mathbf{0})-4\pi\mathcal{J}_D$.

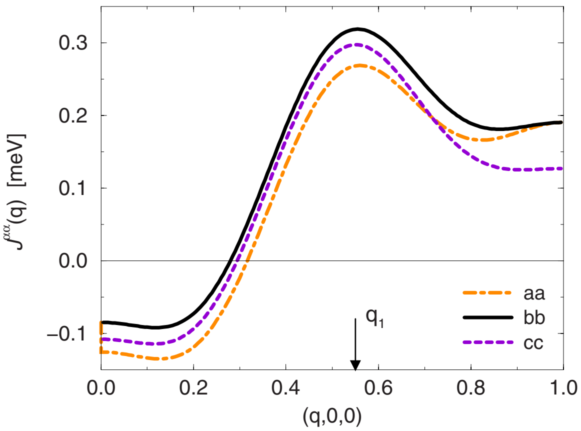

FIG. 1. (Color online) The Fourier transforms of the two-ion interaction components $\mathcal{J}^{\alpha\alpha}(\boldsymbol{q})$ in $GdNi_2B_2C$ for $\boldsymbol{q}$ along [100] and $\alpha=a$, b, or c.

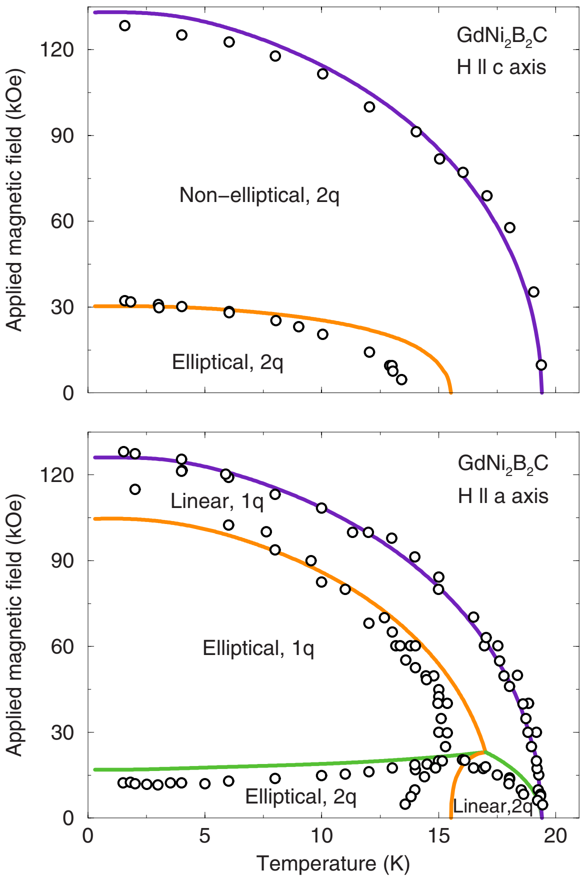

FIG. 2. (Color online) The phase diagrams of $GdNi_2B_2C$, when a field is applied along the a or the c axis. The solid lines are the calculated results obtained for a spherical sample. The circles show the results obtained from magnetization and magnetostriction measurements by El Massalami *et al.* (Ref. 13).

For a certain starting configuration, the effective mean field acting on each site of the commensurable period is calculated, and the corresponding moment $\langle\boldsymbol{J}_i\rangle$ determined by the Brillouin function. The calculation is then carried through with the new configuration of moments, which whole procedure is repeated until self-consistency is attained.

III. THEORETICAL RESULTS AND COMPARISONS WITH EXPERIMENTS

The calculated phase diagrams obtained, when applying a field along [100] and along [001], are compared with the experimental results of El Massalami *et al.*[13] in Fig. 2. Just below T_N, the a-axis phase diagram is in accordance with the results derived from the Landau expansion. As the temperature is reduced, the maximum length of the linearly polarized oscillating moments approaches the saturation value and higher-order odd harmonics are developed. Below $T_R \simeq 13.6$ K, it becomes energetically favorable to reduce these

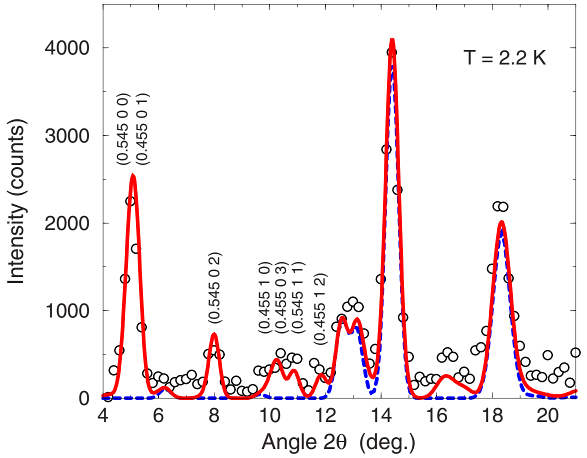

FIG. 3. (Color online) Neutron-diffraction pattern from powder of $GdNi_2B_2C$ at $T=2.2$ K. Symbols show the experimental data taken from Rotter *et al.* (Ref. 11). The dashed line indicates a fit of the nuclear pattern observed at $T=30\ K>T_N$. The solid line shows the result of adding the calculated magnetic scattering intensities to the fit of the nuclear ones. The magnetic peak intensities are those derived from the stable asymmetric double-q structure described in the text.

higher harmonics by the establishment of an elliptical polarization. Assuming the major (first harmonic) part of the ordered moments in the a-b plane to be given by Eq. (6), then the corresponding c component appearing below T_R is

$$\langle \boldsymbol{J}_i \cdot \hat{\boldsymbol{c}} \rangle = m_{c2} \sin(\boldsymbol{q}_2 \cdot \boldsymbol{r}_i + \phi_a) + m_{c1} \sin(\boldsymbol{q}_1 \cdot \boldsymbol{r}_i + \phi_b). \tag{10}$$

As noticed by Detlefs *et al.*,[10] the similar transition, in the single-q case, is also observed in Er metal.[22] The "squaring-up" process is weaker than that in the single-q case, and the phase diagram indicates that the double-q ordering reduces this transition temperature by nearly 2 K compared to the single-q case. If the elliptical polarization was shared equally by the two single-q components ($m_{c1}=m_{c2}$ and $m_a=m_b$), the transition would be of second order, but in the present model and several related ones, the symmetric structure is only metastable. In the stable structure, only one of the two single-q components is elliptically polarized, whereas the other slightly smaller component stays (nearly) linearly polarized. In this structure, the a and b directions are no longer equivalent and the transition to the elliptically polarized phase becomes of first order, although it is very close to be continuous at zero field in the final model.

The calculated magnetic structure at low temperatures has been used to generate a neutron-diffraction pattern, which is compared to experimental data in Fig. 3. The result derived from the model is in good agreement with the data, if the experimental error involved in scattering experiments using hot neutrons is taken into account. The specific heat derived from the model is compared with the experimental results of Godart *et al.*[23] in Fig. 4. The two transition temperatures at zero field determined from this experiment, $T_N \simeq 20$ K and $T_R \simeq 13.5$ K, agree with those determined from the results of El Massalami *et al.*[13] shown in Fig. 2. The specific heat derived from the mean-field model does not account for the relatively large critical magnetic contributions observed above T_N; however, the steps in the heat capacity calculated at the two transitions are of the right order of magnitude.

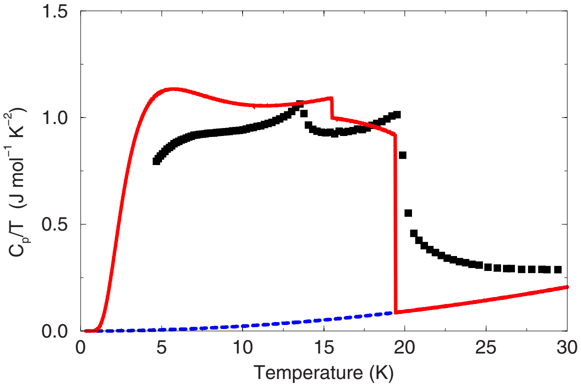

FIG. 4. (Color online) The experimental results for the specific heat shown by the solid squares have been obtained by Godart *et al.* (Ref. 23) The solid line shows the total of the magnetic contribution and that derived from a Debye model with $\theta_D=370$ K. The phonon contribution is indicated by the dashed line below T_N.

When applying a field along the a axis, the domain in which the elliptically polarized moments are perpendicular to the field is favored by the field, and the other double-q component of this structure vanishes at the relatively low field of 10–20 kOe. In the case where the field is applied along the c axis, the field does not affect the stability of the double-q arrangement, but the elliptical polarization is removed well below the field at which the antiferromagnetic ordering is destroyed. The phase at intermediate fields in the c-axis phase diagram is named "nonelliptical 2q" in Fig. 2 since the c-axis component of the moments is still modulated at the even harmonics of $\boldsymbol{q}_1$ or $\boldsymbol{q}_2$ (and at linear combinations of the two wave vectors). Hence, the transition from the "elliptical" to the "nonelliptical" phase is characterized by the disappearance of the two first harmonics (and the higher-order odd ones) in the spatial variation of the c-axis moments, which gives rise to a kink in the magnetization curve as observed experimentally.[13]

If the elliptical polarization were equally shared by the two single-q components at low temperatures, the double-q configuration would not lead to any orthorhombic distortion of the tetragonal a-b plane at zero field. However, in spite of the asymmetry predicted by the present model, the correlation function introduced by Eq. (3) accounts acceptably for the orthorhombic distortion $\epsilon_a - \epsilon_b$ induced by the a-axis field. The calculated correlation function is compared with the experimental strain variation observed at 2 K by Rotter *et al.*[11] in Fig. 5.

IV. CONCLUSION

The mean-field analysis shows that the magnetic moments in $GdNi_2B_2C$ are ordered in a double-q structure below T_N at zero field. The only discrepancy of some importance, be-

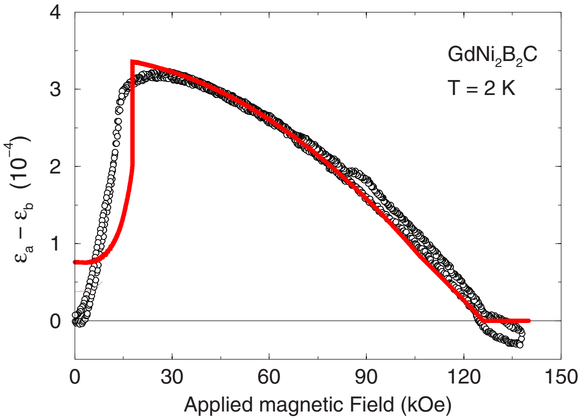

FIG. 5. (Color online) The field dependence of the orthorhombic distortion $\epsilon_a - \epsilon_b$ of GdNi$_2$B$_2$C at 2 K. The experimental results are from Rotter *et al.* (Ref. 11) and are compared with the calculated correlation function introduced on the rhs of Eq. (3) scaled by the factor 1.44×10^{-5}.

tween the theoretical phase diagram and experiments, is that T_R is predicted to be about 2 K higher than observed, which also applies to the tetracritical point in the a-axis phase diagram. The exchange interaction parameters derived in the analysis are subjected to some arbitrariness. However, $\mathcal{J}^{bb}(\boldsymbol{q})$ at zero and at the ordering wave vector are well determined and, in addition, we have found that it is important that $\mathcal{J}^{bb}(\boldsymbol{q})$ has a sharp maximum at the ordering wave vector. The sharp maximum is needed in order to prevent a larger reduction of the length of the ordering wave vector when the temperature is reduced. A strong reduction would be in contradiction with the tendency of a small increase of this length seen experimentally.[10] The situation is equivalent to the one occurring in the case or Er borocarbide,[7] and although $\mathcal{J}^{bb}(\boldsymbol{q})$ in Fig. 1 is strongly peaked at $\boldsymbol{q}=\boldsymbol{q}_1$, the calculated length of the ordering wave vector is still being reduced, but only by a few percent, from 5/9 at T_N to about 6/11 of a^* at zero temperature, when assuming the ordering wave vectors to be along the $\langle 100 \rangle$ directions. At the lowest temperatures, the true free-energy minimum of the present mean-field model is found to be determined by the planar double-q structure,

$$\begin{cases} \langle J_{ia} \rangle = J_0 \cos(\boldsymbol{q}_2' \cdot \boldsymbol{r}_i + \phi), & \boldsymbol{q}_2' = \left(\pm\xi, \tfrac{1}{2} + \xi, 0\right) \\ \langle J_{ib} \rangle = J_0 \sin(\boldsymbol{q}_1' \cdot \boldsymbol{r}_i + \phi), & \boldsymbol{q}_1' = \left(\tfrac{1}{2} + \xi, \pm\xi, 0\right), \end{cases} \tag{11}$$

where $\xi \simeq 0.036$ (here, we neglect a minute rotation of the structure due to the classical interaction). This structure has the remarkable property that $|\boldsymbol{J}_i| = J_0$ at all sites for an arbitrary value of ξ ($\pm\xi$ should be read either as $+\xi$ or $-\xi$ in both wave vectors). Hence, this particular double-q structure may maximize $|\boldsymbol{J}_i|$ with no need for incorporating higher harmonics or a c-axis component. This property means that the structure may be able to compensate for the smaller value of $\mathcal{J}^{bb}(\boldsymbol{q})$ at $\boldsymbol{q}_1'$ in comparison with the double-q structure at $(\boldsymbol{q}_1, \boldsymbol{q}_2)$ since the latter one is going to involve a nonzero c-axis component and higher harmonics, when $|\boldsymbol{J}_i|$ is close saturation. Experimentally,[10] the c-axis component increases steadily as the temperature is reduced, indicating that the planar structure in Eq. (11) does not appear. In order to destabilize it in the model calculations, the maximum in $\mathcal{J}^{bb}(\boldsymbol{q})$ needs to be more sharp, at least in the direction perpendicular to $\boldsymbol{q}_1$.

The present analysis has general implications. The precise locations of the phase lines depend on the specific model parameters, but the Landau expansion indicates that the double-q ordering is going to occur in all Gd compounds sharing the present symmetries. The requirement is only that (i) the possible set of linearly polarized single-q structures should contain a pair where the polarization vectors make an angle of between $\frac{\pi}{3}$ and $\frac{2\pi}{3}$ with each other and (ii) that the different two-ion interaction components are nondegenerate at the ordering wave vector. Since the occurrence of the double-q ordering strongly reduces the orthorhombic distortion anticipated for a single-q antiferromagnet, the present mechanism resolves the magnetoelastic paradox of GdNi$_2$B$_2$C and has the potential for doing the same in the case of other (planar ordered, tetragonal) Gd compounds.

If the fourth-order term of Er or Tb borocarbide were not modified by anisotropic crystal-field terms, they should also show a double-q ordering. However, here the magnetoelastic energy of the orthorhombic distortion is of the order of hundred times larger than that in GdNi$_2$B$_2$C and is favoring a single-q ordering, which is also the case with the four-state clock anisotropy shown by the two compounds. The orthorhombic distortion is observed to appear immediately below T_N at zero field in both compounds,[24,25] which is a strong indicator of a single-q ordering. Nevertheless, the metastable domain of ErNi$_2$B$_2$C, when placed in the a-axis field, is observed to reappear in a reversible way at decreasing values of the field,[8,26] suggesting that the two single-q domains in this system do interfere with each other.

ACKNOWLEDGMENTS

Brigitte Beuneu and Alexander Barcza are gratefully acknowledged for very fruitful discussions and for their constructive advice with respect to the interpretation of the neutron scattering data. We thank Herwig Michor for providing us with the numerical data for the specific heat.

---

[1] M. Rotter, M. Loewenhaupt, M. Doerr, A. Lindbaum, H. Sassik, K. Ziebeck, and B. Beuneu, Phys. Rev. B **68**, 144418 (2003).

[2] J. Jensen and A. R. Mackintosh, *Rare Earth Magnetism: Structures and Excitations* (Clarendon, Oxford, 1991).

[3] K.-H. Müller and V. N. Narozhnyi, Rep. Prog. Phys. **64**, 943 (2001).

[4] L. C. Gupta, Adv. Phys. **55**, 691 (2006).

[5] J. W. Lynn, S. Skanthakumar, Q. Huang, S. K. Sinha, Z. Hossain,

L. C. Gupta, R. Nagarajan, and C. Godart, Phys. Rev. B **55**, 6584 (1997).

[6] B. J. Suh, F. Borsa, D. R. Torgeson, B. K. Cho, P. C. Canfield, D. C. Johnston, J. Y. Rhee, and B. N. Harmon, Phys. Rev. B **53**, R6022 (1996).

[7] J. Jensen, Phys. Rev. B **65**, 140514(R) (2002).

[8] A. Jensen, K. Nørgaard Toft, A. B. Abrahamsen, D. F. McMorrow, M. R. Eskildsen, N. H. Andersen, J. Jensen, P. Hedegård, J. Klenke, S. Danilkin, K. Prokes, V. Sikolenko, P. Smeibidl, S. L. Bud'ko, and P. C. Canfield, Phys. Rev. B **69**, 104527 (2004).

[9] N. H. Andersen, J. Jensen, T. B. S. Jensen, M. v. Zimmermann, R. Pinholt, A. B. Abrahamsen, K. Nørgaard Toft, P. Hedegård, and P. C. Canfield, Phys. Rev. B **73**, 020504(R) (2006).

[10] C. Detlefs, A. I. Goldman, C. Stassis, P. C. Canfield, B. K. Cho, J. P. Hill, and D. Gibbs, Phys. Rev. B **53**, 6355 (1996).

[11] M. Rotter, A. Lindbaum, A. Barcza, M. El Massalami, M. Doerr, M. Loewenhaupt, H. Michor, and B. Beuneu, Europhys. Lett. **75**, 160 (2006).

[12] S. B. Dugdale, M. A. Alam, I. Wilkinson, R. J. Hughes, I. R. Fisher, P. C. Canfield, T. Jarlborg, and G. Santi, Phys. Rev. Lett. **83**, 4824 (1999).

[13] M. El Massalami, H. Takeya, H. Hirata, M. Amara, R.-M. Galera, and D. Schmitt, Phys. Rev. B **67**, 144421 (2003).

[14] A. Lindbaum and M. Rotter, in *Handbook of Magnetic Materials*, edited by K. H. J. Buschow (Elsevier, Amsterdam, 2003), Vol. 14, p. 307.

[15] A. B. Harris and J. Schweizer, Phys. Rev. B **74**, 134411 (2006).

[16] E. M. Forgan, J. Phys. F: Met. Phys. **12**, 779 (1982).

[17] http://www.mcphase.de

[18] M. Rotter, M. Doerr, and M. Loewenhaupt, J. Appl. Phys. **91**, 8885 (2002).

[19] M. Rotter, A. Schneidewind, M. Doerr, M. Loewenhaupt, A. M. El Massalami, and C. Detlefs, Physica B **345**, 231 (2004).

[20] M. Rotter, J. Magn. Magn. Mater. **272-276**, 481 (2004).

[21] K. A. McEwen and M. B. Walker, Phys. Rev. B **34**, 1781 (1986).

[22] R. A. Cowley and J. Jensen, J. Phys.: Condens. Matter **4**, 9673 (1992); J. Jensen and R. A. Cowley, Europhys. Lett. **21**, 705 (1993).

[23] C. Godart, I. Felner, H. Michor, G. Hilscher, E. Tominez, and E. Alleno, J. Alloys Compd. **275-277**, 642 (1998).

[24] C. Detlefs, A. H. M. Z. Islam, T. Gu, A. I. Goldman, C. Stassis, P. C. Canfield, J. P. Hill, and T. Vogt, Phys. Rev. B **56**, 7843 (1997).

[25] C. Song, Z. Islam, L. Lottermoser, A. I. Goldman, P. C. Canfield, and C. Detlefs, Phys. Rev. B **60**, 6223 (1999).

[26] M. Doerr, M. Rotter, M. El Massalami, S. Sinning, H. Takeya, and M. Loewenhaupt, J. Phys.: Condens. Matter **14**, 5609 (2002).